J|A|C|S
ARTICLES
Published on Web 09/12/2002

Synthesis of a Negatively Charged Dibenzofuran-Based β-Turn Mimetic and Its Incorporation into the WW Miniprotein-Enhanced Solubility without a Loss of Thermodynamic Stability

Ramesh Kaul, Songpon Deechongkit, and Jeffery W. Kelly*

Contribution from the Department of Chemistry and The Skaggs Institute of Chemical Biology, The Scripps Research Institute, 10550 North Torrey Pines Road, BCC 506, La Jolla, California 92037

Received May 10, 2002

Abstract: A versatile synthesis has been developed to functionalize the 4-(2-aminoethyl)-6-dibenzofuran propionic acid residue (**1a**) at the 2 and 8 positions with a variety of different substructures. The unfunctionalized version of this peptidomimetic (**1a**) is known to facilitate β-hairpin formation in a variety of small peptides and proteins in aqueous solution when incorporated in place of the $i+1$ and $i+2$ residues of a β-turn. In this study, we append propionate substituents on **1a** at the 2 and 8 positions to successfully overcome solubility problems encountered with the incorporation of **1a** in place of the $i+1$ and $i+2$ residues of the β-turn in loop 1 of the WW domain. The thermodynamic stability of several WW domain analogues incorporating residues **1a** and **1b** was compared to that of the wild-type sequence revealing comparable $\Delta G(H_2O)$ unfolding values at 4 °C ranging from 3 to 3.6 kcal/mol. WW domains incorporating residue **1b** exhibit improved solubility (exceeding 100 μM) and resistance to aggregation without compromising thermodynamic stability.

Introduction

The synthesis, conformational analysis, and activity assessment of peptidomimetics are active research areas for numerous chemists.[1] Peptidomimetics have been used for many applications in medicinal chemistry[2] and more recently in protein chemistry.[3] Most peptidomimetics imitate elements of secondary structure, such as an α-helix, β-strand, β-sheet, and turns of numerous types utilized in biological molecular recognition studies. For the most part, peptidomimetics have been used in lieu of peptide hormones (agonists or antagonists)[4] or as protease inhibitors.[2,5] Peptidomimetics have been increasingly utilized in small proteins as tools to help understand their folding and/or stability or to control their assembly into nanostructures of differing morphology.[3a,e,h,i] While several peptidomimetics have been incorporated into proteins, most were not designed for this application; hence, the solubility of the resulting protein is less

* To whom correspondence should be addressed. Voice: (858) 784-9605. Fax: (858) 784-9610. E-mail: jkelly@scripps.edu.

(1) For recent reviews, see: (a) Bursavich, M. G.; Rich, D. H. *J. Med. Chem.* **2002**, *45*, 541−558. (b) Burgess, K. *Acc. Chem. Res*. **2001**, *34*, 826−835. (c) Hruby, V. J.; Balse, P. M. *Curr. Med. Chem.* **2000**, *7*, 945−970. (d) Ripka, A. S.; Rich, D. H. *Curr. Opin. Chem. Biol.* **1998**, *4*, 439−52. (e) Schneider, J. P.; Kelly, J. W. *Chem. Rev.* **1995**, *95*, 2169−87. (f) Smith, A. B., III; Guzman, M. C.; Sprengeler, P. A.; Keenan, T. P.; Holcomb, R. C.; Wood, J. L.; Carroll, P. J.; Hirschmann, R. *J. Am. Chem. Soc*. **1994**, *116*, 9947−9962. (g) Hirschmann, R. *Angew. Chem., Int. Ed. Engl*. **1991**, *30*, 1278−1301. (h) Kemp, D. S. *Trends Biotechnol*. **1990**, *8*, 249−55. (i) Chorev, M.; Goodman, M. *Acc. Chem. Res*. **1993**, *26*, 266−73.

(2) For examples, see: (a) Ghosh, A. K.; Bilcer, G.; Schiltz, G. *Synthesis* **2001**, *15*, 2203−29. (b) Muller, G. *Top. Curr. Chem.* **2001**, *211*, 17−59. (c) Porter, E. A.; Wang, X.; Lee, H.-S.; Weisblum, B.; Gellman, S. H. *Nature* **2000**, *404*, 565. (d) Mimoto, T.; Kato, R.; Takaku, H.; Nojima, S.; Terashima, K.; Misawa, S.; Fukazawa, T.; Ueno, T.; Sato, H.; Shintani, M.; Kiso, Y.; Hayashi, H. *J. Med. Chem*. **1999**, *42*, 1789−802. (e) Smith, A. B., III; Hirschmann, R.; Pasternak, A.; Yao, W.; Sprengeler, P. A.; Holloway, K. M.; Kuo, L. C.; Chen, Z.; Darke, P. L.; Schleif, W. A. *J. Med. Chem.* **1997**, *40*, 2440−4. (f) De Lucca, G. V.; Erickson-Viitanen, S.; Lam, P. Y. S. *Drug Discovery Today* **1997**, *2*, 6−18. (g) Beaulieu, P. L.; Wernic, D.; Abraham, A.; Anderson, P. C.; Bogri, T.; Bousquet, Y.; Croteau, G.; Guse, I.; Lamarre, D.; Liard, F.; Paris, W.; Thibeault, D.; Pav, S.; Tong, L. *J. Med. Chem.* **1997**, *40*, 2164−76. (h) Kiso, Y. *Biopolymers* **1996**, *40*, 235−244. (i) Larder, B. A.; Hertogs, K.; Bloor, S.; van den Eynde, Ch.; DeCian, W.; Wang, Y.; Freimuth, W. W.; Tarpley, G. *AIDS (London)* **2000**, *14*, 1943−8. (j) Adang, A. E. P.; Hermkens, P. H. H.; Linders, J. T. M.; Ottenheijm, H. C. J.; van Staveren, C. J. *Recl. Trav. Chim. Pays-Bas* **1994**, *113*, 63−78.

(3) (a) Kaul, R.; Angeles, A. R.; Jaeger, M.; Powers, E. T.; Kelly, J. W. *J. Am. Chem. Soc*. **2001**, *123*, 5206−5212. (b) Cheng, R. P.; Gellman, S. H.; DeGrado, W. F. *Chem. Rev.* **2001**, *101*, 3219−3232. (c) Pellegrini, M. C.; Liang, H.; Mandiyan, S.; Wang, K.; Yuryev, A.; Vlattas, I.; Sytwu, T.; Li, Y. C.; Wennogle, L. P. *Biochemistry* **1998**, *37*, 15598−606. (d) Beligere, G. S.; Dawson, P. E. *J. Am. Chem. Soc*. **2000**, *122*, 12079−82. (e) Lashuel, H. A.; LaBrenz, S. R.; Woo, L.; Serpell, L. C.; Kelly, J. W. *J. Am. Chem. Soc*. **2000**, *122*, 5262−77. (f) Short, G. F., III; Golovine, S. Y.; Hecht, S. M. *Biochemistry* **1999**, *38*, 8808−19. (g) Cload, S. T.; Liu, D. R.; Froland, W. A.; Schultz, P. G. *Chem. Biol*. **1996**, *3*, 1033−8. (h) Choo, D. W.; Schneider, J. P.; Graciani, N. R.; Kelly, J. W. *Macromolecules* **1996**, *29*, 355−66. (i) Ghadiri, M. R.; Granja, J. R.; Milligan, R. A.; McRee, D. E.; Khazanovich, N. *Nature* **1993**, *366*, 324−7.

(4) For examples, see: (a) Nargund, R. P.; Patchett, A. A.; Bach, M. A.; Murphy, M. G.; Smith, R. G. *J. Med. Chem*. **1998**, *41*, 3103−3127. (b) Tong, Y.; Olczak, J.; Zabrocki, J.; Gershengorn, M. C.; Marshall, G. R.; Moeller, K. D. *Tetrahedron* **2000**, *56*, 9791−800. (c) Bhatt, U.; Just, G. *Helv. Chim. Acta* **2000**, *83*, 722−7. (d) Yang, L.; Berk, S. C.; Rohrer, S. P.; Mosley, R. T.; Guo, L.; Underwood, D. J.; Arison, B. H.; Birzin, E. T.; Hayes, E. C.; Mitra, S. W.; Parmar, R. M.; Cheng, K.; Wu, T.-J.; Butler, B. S.; Foor, F.; Pasternak, A.; Pan, Y.; Silva, M.; Freidinger, R. M.; Smith, R. G.; Chapman, K.; Schaeffer, J. M.; Patchett, A. A. *Proc. Natl. Acad. Sci. U.S.A.* **1998**, *95*, 10836−41. (e) Hirschmann, R.; Nicolaou, K. C.; Pietranico, S.; Leahy, E. M.; Salvino, J.; Arison, B.; Cichy, M. A.; Spoors, P. G.; Shakespeare, W. C. *J. Am. Chem. Soc*. **1993**, *115*, 12550−68. (f) Veber, D. F.; Holly, F. W.; Paleveda, W. J.; Nutt, R. F.; Bergstrand, S. J.; Torchiana, M.; Glitzer, M. S.; Saperstein, R.; Hirschmann, R. *Proc. Natl. Acad. Sci. U.S.A.* **1978**, *75*, 2636−40.

10.1021/ja020675x CCC: $22.00

than ideal, making it difficult to characterize these systems. Functionalized peptidomimetics that enhance protein solubility without compromising thermodynamic stability would be desirable.

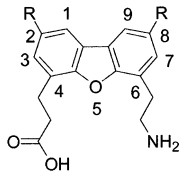

1

1a, R=H

1b, R=$(CH_2)_2$-COOH

Our group has developed the 4-(2-aminoethyl)-6-dibenzofuran propionic acid residue (**1a**) as a β-turn mimetic that facilitates β-hairpin formation in small peptides by replacing the $i + 1$ and $i + 2$ residues of a β-turn, but does not attempt to duplicate the orientation of the $i + 1$ and $i + 2$ side chains.[6d−g] In an effort to extend these studies to proteins amenable to thermodynamic analysis, we developed a practical synthesis of a more soluble version of **1a**, that is, residue **1b**. We have chosen to incorporate this residue into the PIN WW domain miniprotein comprised of residues 6−39.

WW domains are named after the two conserved W residues spaced 20−22 amino acids apart in their sequence.[7] These three-stranded β-sheet domains, found in more than 200 multidomain proteins, bind peptide ligands often mediating protein−protein interactions.[7] These domains are readily accessible through solid-phase peptide synthesis or by expression in *E. coli* and exhibit two-state folding behavior amenable to detailed kinetic and thermodynamic analyses.[6,8] The crystal structure (1.35 Å resolution) of the two domain PIN1 protein (a mitosis cell cycle regulator)[9] and the NMR structure of the isolated PIN1 WW domain (residues 6−39)[10] demonstrate that the isolated PIN WW domain folds into a three-stranded antiparallel β-sheet conformation irrespective of whether the peptidyl-prolyl cis−trans isomerase domain is present (Figure 1). Extensive kinetic and thermodynamic analyses of several single-site variants of the PIN WW domain reveal that the formation of loop 1 is rate limiting for its folding; hence, we will focus our efforts on making structural analogues of loop 1.[8]

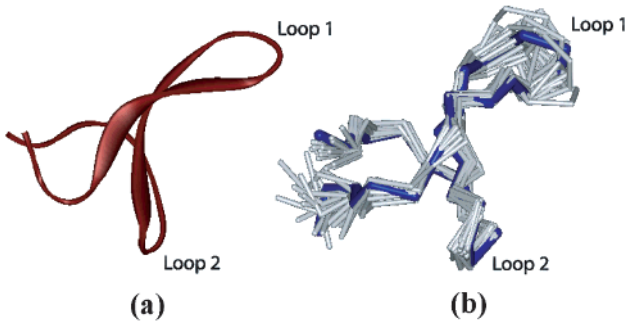

Figure 1. (a) Ribbon diagram of the polypeptide backbone of the isolated WW domain from the PIN1 X-ray crystal structure. (b) Line diagram representation of 20 low energy structures compatible with the NMR constraints for the isolated PIN WW domain (6−39). The blue structure represents the average of the structural ensemble.

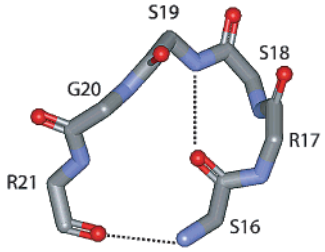

Figure 2. Backbone diagram showing the wt PIN loop 1 (S16 to R21) with the dotted lines representing hydrogen bonds.

Loop 1 (Figure 2) is referred to as a 4:6 loop because it incorporates a type II β-turn near the center of the loop (S16 to S19), having a four-residue hydrogen bond between the C═O of residue 16 and the NH of residue 19 (characteristic of a β-turn), and a six-residue hydrogen bond between the NH of residue 16 and the C═O of residue 21. This loop plays a critical role in binding the phosphoserine (pS) residue in the YSPTpSPS peptide substrate. Recently, we reported that **1a** can be incorporated into loop 1 of the PIN1 WW domain 6−39 miniprotein.[3a] Residue **1a** was designed to replace the $i + 1$ and $i + 2$ residues of a β-turn, that is, residues 17 and 18. We first incorporated **1a** out of context, that is, in place of residues 18 and 19 (peptide **C**), to understand how rigid the conformational requirements of loop 1 are with regard to folding and stability. We found that the thermodynamic stability of the PIN WW domain incorporating **1a** out of context was within 0.5 kcal/mol of wt PIN (6−39) stability, suggesting that the acquisition of native structure can tolerate a non-native sequence and, by extension, a non-native conformation in loop 1. While this WW domain variant having **1a** replacing residues 18 and 19 is monomeric in aqueous buffers, its solubility is not as high as that of the wild-type PIN WW domain. The decreased solubility probably results from replacing the polar S18-S19 dipeptide substructure with the nonpolar dibenzofuran ring system of residue **1a**.

(5) For examples, see: (a) Ripka, A. S.; Satyshur, K. A.; Bohacek, R. S.; Rich, D. H. *Org. Lett.* **2001**, *3*, 2309−12. (b) Dussault, I.; Lin, M.; Hollister, K.; Wang, E. H.; Synold, T. W.; Forman, B. M. *J. Biol. Chem.* **2001**, *276*, 33309−33312. (c) Demarcus, M.; Ganadu, M. L.; Mura, G. M.; Porcheddu, A.; Quaranta, L.; Reginato, G.; Taddei, M. *J. Org. Chem.* **2001**, *66*, 697−706. (d) Shultz, M. D.; Bowman, M. J.; Ham, Y.-W.; Zhao, X.; Tora, G.; Chmielewski, J. *Angew. Chem., Int. Ed.* **2000**, *39*, 2710−2713. (e) Ogilvie, W.; Bailey, M.; Poupart, M.-A.; Abraham, A.; Bhavsar, A.; Bonneau, P.; Bordeleau, J.; Bousquet, Y.; Chabot, C.; Duceppe, J.-S.; Fazal, G.; Goulet, S.; Grand-Maitre, C.; Guse, I.; Halmos, T.; Lavallee, P.; Leach, M.; Malenfant, E.; O'Meara, J.; Plante, R.; Plouffe, C.; Poirier, M.; Soucy, F.; Yoakim, C.; Deziel, R. *J. Med. Chem.* **1997**, *40*, 4113−35. (f) Tamura, S. Y.; Shamblin, B. M.; Brunck, T. K.; Ripka, W. C. *Bioorg. Med. Chem. Lett.* **1997**, *7*, 1359−64. (g) Smith, A. B., III; Akaishi, R.; Jones, D. R.; Keenan, T. P.; Guzman, M. C.; Holcomb, R. C.; Sprengeler, P. A.; Wood, J. L. *Biopolymers* **1995**, *37*, 29−53.

(6) (a) Kiick, K. L.; Saxon, E.; Tirrell, D. A.; Bertozzi, C. R. *Proc. Natl. Acad. Sci. U.S.A.* **2002**, *99*, 19−24. (b) Datta, D.; Wang, P.; Carrico, I. S.; Mayo, S. L.; Tirrell, D. A. *J. Am. Chem. Soc.* **2002**, *124*, 5652−3. (c) Cornish, V. W.; Mendel, D.; Schultz, P. G. *Angew. Chem., Int. Ed. Engl.* **1995**, *34*, 621−33. (d) Tsang, K. Y.; Dìaz, H.; Graciani, N.; Kelly, J. W. *J. Am. Chem. Soc.* **1994**, *116*, 3988−4005. (e) Dìaz, H.; Tsang, K. Y.; Choo, D.; Kelly, J. W. *Tetrahedron* **1993**, *49*, 3533−45. (f) Dìaz, H.; Tsang, K. Y.; Choo, D.; Espina, J. R.; Kelly, J. W. *J. Am. Chem. Soc.* **1993**, *115*, 3790−1. (g) Dìaz, H.; Espina, J. R.; Kelly, J. W. *J. Am. Chem. Soc.* **1992**, *114*, 8316−8. (h) Dìaz, H.; Kelly, J. W. *Tetrahedron Lett.* **1991**, *32*, 5725−8.

(7) (a) Macias, M. J.; Gervais, V.; Civera, C.; Oschkinat, H. *Nat. Struct. Biol.* **2000**, *7*, 375−379. (b) Verdecia, M. A.; Bowman, M. E.; Lu, K. P.; Hunter, T.; Noel, J. P. *Nat. Struct. Biol.* **2000**, *7*, 639−643. (c) Sudol, M.; Hunter, T. *Cell* **2000**, *103*, 1001−1004. (d) Sudol, M. *Prog. Biophys. Mol. Biol.* **1996**, *65*, 113−132. (e) Staub, O.; Rotin, D. *Structure* **1996**, *4*, 495−499. (f) Lu, P. J.; Zhou, X. Z.; Shen, M.; Lu, K. P. *Science* **1999**, *283*, 1325−8. (g) Lu, K. P.; Hanes, S. D.; Hunter, T. *Nature* **1996**, *380*, 544−7.

(8) (a) Jäger, M.; Nguyen, H.; Crane, J. C.; Kelly, J. W.; Grüebele, M. *J. Mol. Biol.* **2001**, *311*, 373−393. (b) Ferguson, N.; Johnson, C. M.; Macias, M.; Oschkinat, H.; Fersht, A. *Proc. Natl. Acad. Sci. U.S.A.* **2001**, *98*, 13002−7.

(9) Ranganathan, R.; Lu, K. P.; Hunter, T.; Noel, J. P. *Cell* **1997**, *89*, 875−86.

(10) Kowalski, J. A.; Liu, K.; Kelly, J. W. *Biopolymers* **2002**, *63*, 111−21.

Scheme 1. Strategy for the Synthesis of Side-Chain Protected, Charged Dibenzofuran-Based β-Turn Mimetic (**4**)

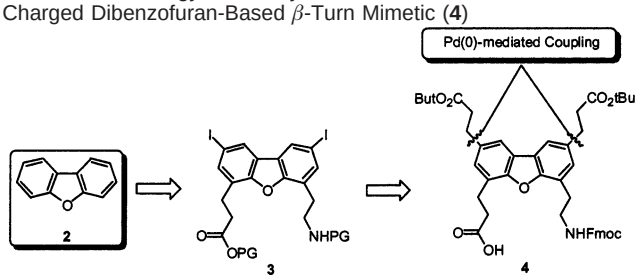

The next logical step of replacing the $i + 1$ (R17) and $i + 2$ (S18) residues of the β-turn in loop 1 with **1a** (i.e., the in context replacement) resulted in an aggregation prone miniprotein, not amenable to characterization. Hence, we could not probe whether the in context replacement would result in a more stable WW domain. Therefore, we synthesized **1b**, a more polar analogue of **1a**, and characterized its solubility and thermodynamic properties both by in context (replacing R17 and S18 with **1b**) and by out of context (replacing S18 and S19 with **1b**) substitutions in the PIN1 WW domain.

Our goal was to prepare a reactive intermediate of residue **1a** that could be functionalized at the 2 and 8 positions with polar substituents enhancing its solubility. Intermediate **3** (Scheme 1) serves this function nicely, allowing a variety of functional groups to be installed in place of the aryl iodide functional groups at positions 2 and 8. As proof of concept, we installed propionic acid appendages at the 2 and 8 positions and demonstrated that WW domains incorporating this residue exhibit superior solubility and very similar thermodynamic stability in cases where direct comparisons are possible with residue **1a**. Substitution at this position could also prove useful for controlling amyloid-like assemblies of peptidomimetics that incorporate **1a**.[3e,h]

Results

***β*-Turn Mimetic Design and Synthesis.** Installation of water-solubilizing groups (propionate groups) at positions 2 and 8 on the dibenzofuran ring system is facilitated by the fact that these positions are selectively reactive toward an electrophilic aromatic iodination reaction. The suitable protected amino acid of **1b** for Fmoc-based solid-phase peptide synthesis is **4**, where the propionate groups and the amino group were protected as *tert*-butyl esters and as Fmoc, respectively, Scheme 1. *tert*-Butyl propionate side chains are attached to the dibenzofuran ring system via a palladium-mediated coupling reaction between 4,6-difunctionalized-2,8-diiododibenzofuran (**12**) and *tert*-butyl acrylate, followed by hydrogenation of the acrylate double bond, Scheme 2. The synthesis of amino acid **4**, described in more detail below, is incorporated into the WW domain sequence by solid-phase peptide synthesis using a strategy compatible with the Fmoc protecting group. The side-chain protecting groups on the α-amino acid residues as well as the 2,8-*tert*-butyl ester protecting groups on residue **4** are removed by TFA deprotection, liberating a β-turn mimic within the WW domain bearing two propionic acid side chains. Therefore, the solubility should be enhanced above the pK_a of these side chains.

The synthesis of **4** commences with iodination of dibenzofuran (**2**), Scheme 2. The regioselectivity of this reaction resulted in iodination at positions 2 and 8, affording **5**. The iodo groups of **5** were converted to the much less reactive trimethylsilyl group using lithiation followed by treatment with trimethylsilyl chloride (TMS-Cl), a group that can be transformed to an iodide later on.[11] Furan oxygen-directed metalation at the 4 and 6 positions followed by halogenation with I_2 affords **7**, a 4,6-diododibenzofuran with trimethylsilyl groups at positions 2 and 8.

Positions 4 and 6 were differentially functionalized by successive Heck reactions.[12] First, **7** underwent a palladium-mediated Heck reaction with ethylacrylate. The monosubstituted product, **8**, was obtained along with some disubstituted product. Thus, the overall yield was moderate (55−60%); however, unreacted **7** can be recycled. Compound **8** was subjected to a second Heck reaction utilizing acrylic acid, affording **9** in 90% yield. The double bonds of **9** were then hydrogenated yielding **10**. A Curtius rearrangement[13] initiated by diphenylphosphoryl azide (DPPA) treatment transformed the carboxylic acid functional group into a carbobenzyloxy carbonyl (*Z*)-protected amino group. Compound **11** was transformed to the key intermediate **12** by treating the trimethylsilyl groups with iodochloride, triethylamine, and carbon tetrachloride, converting them to reactive aryl iodide functionalities.

Key intermediate **12** was subjected to a tandem Heck reaction with *tert*-butyl acrylate to afford **13**. The *tert*-buyl ester protecting group was chosen because it is not removed during the Fmoc solid-phase peptide synthesis conditions required to incorporate **4** into the WW domain, but it is removed by the final TFA treatment which also removes the side-chain protecting groups from the α-amino acid residues. Compound **13** was converted to final product **4** by hydrolysis of the ethyl ester under basic conditions,[14] removal of the *Z*-protecting group using hydrogenation conditions that also convert the alkene in the side chains to alkanes, and, finally, by Fmoc protection of the amino group.[15] The overall synthesis of **4** is outlined in Scheme 2.

PIN1 WW Domain Design. Our group has been studying the thermodynamics and kinetics of PIN1 WW domain folding. The solution and solid-state structures of the WW domain are very similar as demonstrated by the 1.35 Å crystal structure of the WW domain portion of PIN1 (shown in Figure 1a) and the NMR solution structure of the isolated PIN WW (shown in Figure 1b). The formation of loop 1, intervening between strands 1 and 2, is rate limiting for the folding of the PIN WW domain.[8a] Therefore, we have focused on incorporating the dibenzofuran-based β-turn mimetic at strategic locations within loop 1, a six-residue 4:6 β-bulge loop defined by residues S16 to R21, Figure 2. β-Turn mimetics **1a** and **1b** were designed to replace the $i + 1$ and $i + 2$ residues of a β-turn; thus, residues **1a** and **1b** can be incorporated into the WW domain in and out of context with respect to the $i + 1$ and $i + 2$ residues (R17 and S18) of the type II β-turn within loop 1 (**1b** incorporation can be accomplished using its side-chain protected form, **4**, during solid-phase peptide synthesis). As a result, the $i + 1$ and $i + 2$ residues (R17 and S18) and the $i + 2$ and $i + 3$ residues (S18 and S19)

(11) Stock, L. M.; Spector A. R. *J. Org. Chem.* **1963**, *28*, 3272−4.
(12) (a) LaBrenz, S. R.; Bekele, H.; Kelly, J. W. *Tetrahedron* **1998**, *54*, 8671−8678. (b) Beletskaya, I. P.; Cheprakov, A. V. *Chem. Rev.* **2000**, *100*, 3009−66.
(13) Takayuki, S.; Kunihiro, N.; Shunichi, Y. *J. Am. Chem. Soc.* **1972**, *94*, 6203−5.
(14) Corey, E. J.; Szekely, I.; Shiner, C. S. *Tetrahedron Lett.* **1977**, *18*, 3529−32.
(15) Milton, R. C. de L.; Becker, E.; Milton, S. C. F.; Baxter, J. E. J.; Elsworth, J. F. *Int. J. Pept. Protein Res.* **1987**, *30*, 431−2.

Scheme 2. Synthesis of Side-Chain Protected, Charged Dibenzofuran-Based β-Turn Mimetic (**4**)[a]

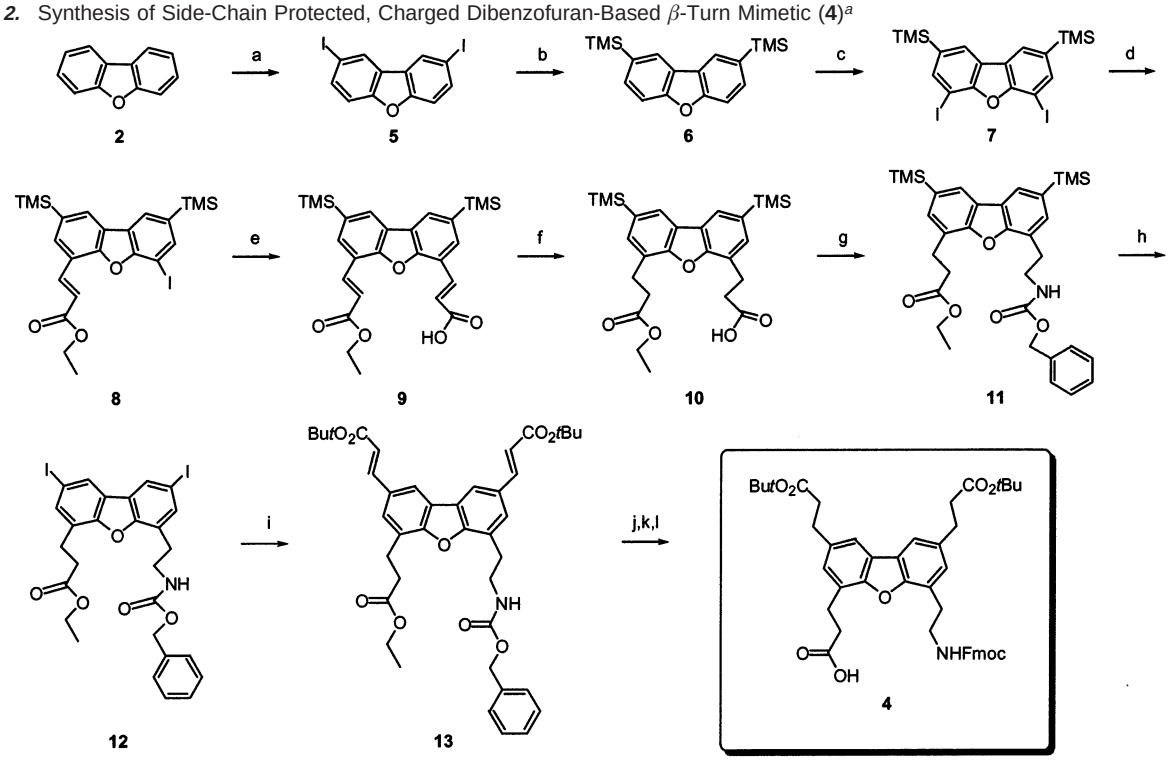

[a] Reagents: (a) I_2, HNO_3, AcOH, H_2SO_4, H_2O, CCl_4 (70%); (b) *tert*-BuLi, THF-ethyl ether, TMSCl, −78 °C (95%); (c) *sec*-BuLi, TMEDA, I_2, ethyl ether (70%); (d) ethylacrylate, $Pd(OAc)_2$, P(*o*-Tolyl)$_3$, Et_3N, DMF, 80 °C (55−60%); (e) acrylic acid, $Pd(OAc)_2$, P(*o*-Tolyl)$_3$, Et_3N, DMF, 80 °C (90%); (f) 10 mol % Pd/C, H_2 (50 psi) (100%); (g) DPPA, BnOH, Et_3N (70%); (h) ICl, CCl_4, $Na_2S_2O_3$ 0 °C (95%); (i) *tert*-butylacrylate, $Pd(OAc)_2$, P(*o*-Tolyl)$_3$, Et_3N, DMF, 80 °C (80%); (j) LiOH, THF:EtOH:H_2O; (k) 10 mol % Pd/C, H_2 (50 psi); (l) Fmoc-OSu 95% three steps.

Table 1. Nomenclature and Sequences for Variants of the PIN WW Domain

		sequences		
peptides	mutations	6	16 - - - loop 1 - - - 21	39
wt PIN		K L P P G W E K R M	*S R S S G R*	V Y Y F N H I T N A S Q W E R P S G
Peptide **A**	R17S18to**1a**	K L P P G W E K R M	*S* **1a** *S G R*	V Y Y F N H I T N A S Q W E R P S G
Peptide **B**	R17S18to**1b**	K L P P G W E K R M	*S* **1b** *S G R*	V Y Y F N H I T N A S Q W E R P S G
Peptide **C**	S18S19to**1a**	K L P P G W E K R M	*S R* **1a** *G R*	V Y Y F N H I T N A S Q W E R P S G
Peptide **D**	S18S19to**1b**	K L P P G W E K R M	*S R* **1b** *G R*	V Y Y F N H I T N A S Q W E R P S G

Table 2. Molecular Weights of PIN WW Domain Variants Obtained by Mass Spectrometry and Sedimentation Equilibrium Analytical Ultracentrifugation

polypeptide	expected mass	observed mass	hydrodynamic weight
wt PIN	4005.5	4006.4	3900 ± 200
Peptide **A**	4045.6	4046.1	n.d.
Peptide **B**	4189.7	4190.1	4342 ± 145
Peptide **C**	4114.6	4114.0	4227 ± 179
Peptide **D**	4258.7	4258.9	4460 ± 119

were substituted by **1a** and **1b**. The out of context substitution at positions *i* and *i* + 1 (S16 and R17) was avoided because S16 is also part of β-strand 1. The sequence of the wild-type PIN WW domain and sequences synthesized by Fmoc solid-phase methods incorporating both β-turn mimetics as well as the nomenclature used are shown in Table 1. All of the proteins were characterized by ESI-MS to confirm their identity (Table 2).

Biophysical Studies. There are two important issues to be addressed by the data outlined in this paper: aqueous solubility and thermodynamic stability of these variants. In this study, aqueous solubility is defined in an operational sense as discerned by the ability of the protein to remain monomeric and soluble at the micromolar concentrations required for biophysical studies. This property is best evaluated by sedimentation equilibrium analytical ultracentrifugation experiments. Table 2 summarizes the hydrodynamic weight of all of the proteins studied herein, which fit best to a single species model of the monomer. Peptide **A** was problematic owing to aggregation and thus does not fit to a monomeric single species model in solution. As a result, thermodynamic analysis was performed on all variants except for Peptide **A**.

Far-UV circular dichroism spectroscopy was used to evaluate whether the constructs were folded and to determine their denaturation curves. Wavelength scans of all of the variants afforded very similar spectra, distinguished by the maximum at 227 nm characteristic of folded WW domains, Figure 3. Thermodynamic stability of all variants was assessed by both thermal and GdHCl-induced denaturation (see Experimental Section).[16] The temperature at the midpoint of denaturation was obtained by thermal denaturation, while $\Delta G(H_2O)$ unfolding at

(16) (a) Gursky, O.; Atkinson, D. *Biochemistry* **1998**, *37*, 1283−91. (b) Sinha, A.; Yadav, S.; Ahmad, R.; Ahmad, F. *Biochem. J.* **2000**, *345*, 711−7. (c) Pace, C. N.; Scholtz, J. M. In *Protein Structure*; Creighton, T. E., Ed.; IRL Press: Oxford, U.K., 1997; pp 299−321. (d) Liskin, S.; Robertson, A. D. *Protein Sci.* **1993**, *2*, 2037−49.

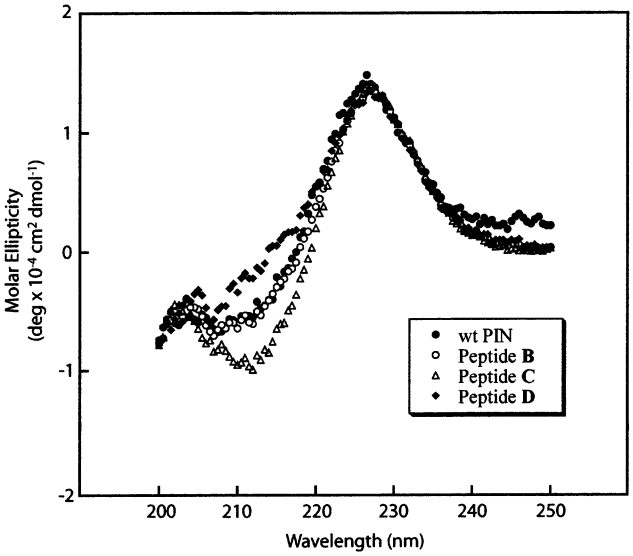

Figure 3. Far-UV CD spectra of wt PIN (●), Peptide **B** (○), Peptide **C** (△), and Peptide **D** (♦) at pH 7 (20 μM sodium phosphate buffer, 2 °C).

Table 3. Aqueous Solubility and Unfolding Thermodynamics of PIN WW Domain Variants

protein	aqueous solubility	T_m (°C)	$\Delta G_{unfolding}$ (kcal/mol) at 4 °C
wt PIN	yes	59	3.3
Peptide **A**	aggregate	n.d.	n.d.
Peptide **B**	yes	48	3.1
Peptide **C**	yes	48	3.6
Peptide **D**	yes	49	3.0

4 °C was obtained by through GdHCl denaturation curves. Table 3 summarizes the thermodynamic parameters characterizing these variants.

Discussion

The synthesis of a side-chain protected β-turn mimetic, **4**, is useful in that it resulted in a more soluble charged β-turn mimetic after deprotection and is versatile in that the functionalized aromatic diiodide **12** can be treated with a wide variety of reactants to create β-turn mimetics with diverse functional groups at the 2 and 8 positions. The charged substituents are incorporated at positions 2 and 8 because these positions are remote from the 4,6 substituents utilized to incorporate this residue into the backbone of a peptide or protein.

The sedimentation equilibrium analytical ultracentrifugation data on WW domains incorporating residues **1a** and **1b** were revealing. Peptide **A**, the in context WW variant incorporating residue **1a**, rapidly aggregated and was insoluble in aqueous buffers, whereas the out of context **1a** substitution (Peptide **C**) was soluble and monomeric. Several approaches were attempted to solubilize Peptide **A** without success. Both the in and the out of context substitutions (Peptide **B** and Peptide **D**, respectively) proved to be soluble and monomeric when residue **1b** was utilized in place of **1a** in the WW domains. Concentrations of WW domains ranging from 20 to 100 μM in 20 μM sodium phosphate buffer at pH 7.0 proved to be soluble.

Because loop 1 is solvent-exposed in both the crystal and the NMR structures, amino acids in the loop likely influence the aggregation state of the domain. The wild-type sequence of loop 1 (residues 16−21, Table 1), composed of mostly polar residues, helps keep the domain monomeric. Modifications in the solvent-exposed loops of proteins are known to affect their aggregation tendency.[17] It is conceivable that incorporation of **1a** into loop 1 generates enough hydrophobic surface to facilitate intermolecular assembly to bury surface area. Incorporation of a more polar amino acid, **1b**, into loop 1 could prevent this problem. Figure 4 shows the solvent accessible surfaces of residues **1a** and **1b**, color-coded by electrostatic potential (generated from Wetlab ViewerLite 4.2 by Accelrys). It is evident from Figure 4 that **1a** displays a hydrophobic surface uninterrupted by polar substructures, whereas **1b** exhibits a hydrophobic surface terminated by negatively charged carboxylates.

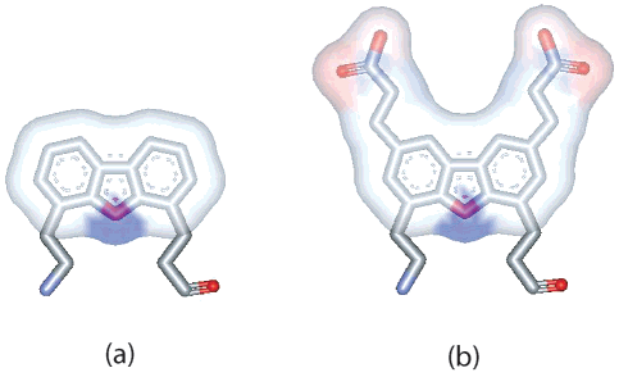

Figure 4. Solvent accessible surface diagrams of (a) neutral β-turn template **1a** and (b) charged β-turn template **1b**. Color scheme corresponds to local charge propensity (red = negative, blue = positive, gray = neutral). Images were generated by ViewerLite 4.2 (Accelrys Inc.).

Even though incorporation of charged substituents on the β-turn mimetic dramatically inhibits aggregation, it did not appreciably change the stability of the resulting WW domains based on chaotrophic denaturation data. All of the peptides studied exhibit $\Delta G(H_2O)$ unfolding values at 4 °C in the range of 3.0−3.6 kcal/mol, demonstrating that they are very similar in stability. All WW domains that incorporate alternative β-turns in loop 1 have a lower midpoint of thermal denaturation (T_m) than that of wt PIN, which is likely a reflection of a change in heat capacity upon unfolding. In fact, it is inappropriate to draw conclusions about protein stability on the basis of T_m data alone. Similarities in the stability of WW domains incorporating residues **1a** and **1b** may be expected, given that the loop region is solvent exposed in both the folded and the unfolded states (desolvation is similar).

Conclusion

The side-chain protected version (**4**) of charged peptidomimetic **1b** can be synthesized in 12 steps in an overall yield of 14% utilizing palladium-mediated Heck couplings and organosilane to iodide transformations as the key steps. β-Turn mimetics were incorporated into loop 1 of the PIN WW domain both in context (R17S18) and out of context (S18S19) with respect to $i + 1$ and $i + 2$ residues of the type II β-turn. The incorporation of the bis-anionic version of the β-turn mimic in lieu of the uncharged analogue resulted in enhanced solubility

(17) (a) Mezo, A. R.; Cheng, R. P.; Imperiali, B. *J. Am. Chem. Soc.* **2001**, *123*, 3885−91. (b) Jappelli, R.; Cesareni, G. *FEBS Lett.* **1996**, *394*, 311−5. (c) Schulze, A. J.; Degryse, E.; Speck, D.; Huber, R.; Bischoff, R. *J. Biotechnol.* **1994**, *32*, 231−8.

without significantly perturbing the thermodynamic stability of the PIN WW domain.

Experimental Section

Materials and Methods. All common organic and inorganic chemicals were purchased from Aldrich Chemical and Fisher Scientific. Anhydrous solvents were purchased from Fisher Scientific and were either used as received or further dried using a Dri-Solv solvent still. Column chromatography was performed with 70-230 mesh silica gel (Fisher Scientific). NMR spectra were acquired on a Bruker DMX 500 MHz spectrometer. ESI-MS were performed on a Hewlett-Packard LC-MS (MSD1100). Uncalibrated melting points were obtained using a Mel-Temp (Laboratory Devices Inc.).

All Fmoc-protected amino acids, Fmoc-Gly-Wang resin (100-200 mesh, 0.7−1.0 mmol/g), 2-(1*H*-benzotriazol-1-yl)-1,1,3,3,-tetramethyluronium hexafluorophosphate (HBTU), and 1-hydroxybenzotriazole (HOBt) were purchased from Novabiochem. Diisopropylethylamine (DIEA), *tert*-butyl methyl ether (MTBE), *m*-cresol, thioanisole, and ethanedithiol (EDT) were purchased from Aldrich Chemical Co. Trifluoroacetic acid was purchased from Advanced Chemtech. Reagent grade dichloromethane (DCM), reagent grade *N*,*N*-dimethylformamide (DMF), and HPLC-grade acetonitrile were purchased from Fisher Scientific. 1-Methyl-2-pyrrolidine (NMP) and all other peptide synthesis reagents were purchased from Applied Biosystems.

Reverse-phase HPLC was performed using Vydac C18 columns employing a Waters HPLC system with model 600 pumps and model 486 or 2487 detectors utilizing 214 and 280 nm UV detection. The flow rate for analytical HPLC was 1 mL/min, while the flow rate for preparative HPLC was 10 mL/min. HPLC solvents employed were 5% acetonitrile, 95% water, 0.1% TFA (solvent A) and 95% acetonitrile, 5% water, 0.1% TFA (solvent B). The purified peptides were identified by ESI-MS. The mass spectrometry data are summarized in Table 2. The peptides were lyophilized and then dialyzed against 20 μM sodium phosphate (pH 7.0). The concentrations of all PIN WW domain variants were determined by UV ($\epsilon_{280} = 13\,940\ M^{-1}\ cm^{-1}$ for non-DBF variants and $\epsilon_{289} = 31\,373\ M^{-1}\ cm^{-1}$ for DBF-incorporated variants).

2,8-Diiododibenzofuran (5). A 500 mL round-bottom flask was charged with 16.8 g (90.1 mmol) of dibenzofuran (**2**), 19.7 g (80 mmol) of iodine, and 7.7 g (44 mmol) of iodic acid. Glacial acetic acid (200 mL), water (15 mL), sulfuric acid (2 mL), and carbon tetrachloride (10 mL) were added to the mixture, and the mixture was heated at 65 °C for 30 h. The desired product (**5**) precipitated as the reaction was cooled to room temperature and was collected by filtration. The precipitate was recrystallized from a hot methanol−benzene mixture to yield 30 g (70%) of **5** as colorless crystals (mp 178−180 °C). HRMS (MALDI-FTMS): calcd for MH^+ 420.9844, found 421.0629. ^{1}H NMR (500 MHz, $CDCl_3$): δ 7.29 (d, $J = 7.1$ Hz, 2H), δ 7.72 (d, $J = 7.1$ Hz, 2H), δ 8.16 (s, 2H). ^{13}C NMR (500 MHz, $CDCl_3$): δ 86.3, 114.0, 125.6, 129.9, 135.6, 155.8.

2,8-Bis-trimethylsilanyl-dibenzofuran (6). A flame-dried 250 mL round-bottom flask was charged with 4.49 g (10.7 mmol) of **5** which was thoroughly purged with argon. Dry THF (50 mL) and dry ether (90 mL) were added by syringe, and the solution was cooled to −78 °C. To the solution was added 42.8 mmol of *tert*-butyllithium (28.5 mL; 1.5 M in pentane) using a syringe pump over 10 min. The mixture was slowly warmed to 0 °C over 5 h and then cooled to −10 °C. Next, 8.0 mL (93.5 mmol) of dry trimethylsilyl chloride was added to the solution by a syringe, and the mixture was stirred at room temperature for 24 h. The solvent was then removed using a rotary evaporator, and the residue was redissolved in dichloromethane. The dichloromethane solution was thoroughly washed with aqueous $NaHSO_3$ to quench the iodine that was liberated during the reaction. Removal of dichloromethane afforded a yellow oil that was purified by flash chromatography on silica gel (hexanes), yielding 3.16 g (95%) of yellow solid which was further recrystallized from methanol to give **6** as long needlelike crystals (mp 98−99 °C). HRMS (GCMS): calcd for MNa^+ 335.1258, found 335.0147. ^{1}H NMR (500 MHz, $CDCl_3$): δ 0.36 (s, 18H), δ 7.55 (d, $J = 6.8$ Hz, 2H), δ 7.59 (d, $J = 6.8$ Hz, 2H), δ 8.14 (s, 2H). ^{13}C NMR (500 MHz, $CDCl_3$): δ 111.4, 124.0, 125.9, 132.3, 134.3, 157.0.

4,6-Diiodo-2,8-bis-trimethylsilanyl-dibenzofuran (7). An oven-dried 250 mL round-bottom flask was purged with nitrogen. Dry diethyl ether (90 mL) and TMEDA (9.1 mL, 60 mmol) were added via syringe, and the solution was cooled to −78 °C. To the solution was added 50 mL (60 mmol) of *sec*-butyllithium (1.2 M in pentane) over 10 min using a syringe pump. After the addition was complete, the mixture was stirred at −78 °C for 10 min, and 6.35 g (20 mmol) of **6** in 50 mL of dry diethyl ether was added by cannula over 10 min. The mixture was stirred at −78 °C for 30 min and then was slowly warmed to room temperature. After 24 h at room temperature, the mixture was cooled to −78 °C, and 25 g (98 mmol) of iodine in 150 mL of dry diethyl ether was added via cannula over 20 min. The mixture was stirred at room temperature for 24 h and then poured into a solution of 120 g of $NaHSO_3$ in 400 mL of water. After collecting the ether, we extracted the aqueous mixture with dichloromethane (3×200 mL). The combined extracts were dried over $MgSO_4$ and concentrated. The resulting yellow crystals were recrystallized from warm dichloromethane−acetonitrile to yield 7.45 g (65%) of **7** as pale yellow crystals (mp 185−188 °C). HRMS (FAB, nitrobenzyl alcohol matrix): calcd for MH^+ 563.9299, found 563.9319. ^{1}H NMR (500 MHz, $CDCl_3$): δ 0.36 (s, 18H), δ 7.26 (s, 2H), δ 7.93 (s, 2H), δ 8.01 (s, 2H). ^{13}C NMR (500 MHz, $CDCl_3$): δ −0.6, 76.6, 124.8, 126.1, 138.0, 141.4, 156.6.

3-(6-Iodo-2,8-bis-trimethylsilanyl-dibenzofuran-4-yl)-acrylic Acid Ethyl Ester (8). An oven-dried 25 mL round-bottom flask was charged with 6.4 g (11.6 mmol) of **7**, 1.06 g (3.6 mmol) of tri-*o*-tolylphosphine, and 0.26 g (1.16 mmol) of palladium(II)acetate, and the flask was purged with nitrogen. Eleven grams (68 mmol) of ethyl acrylate, 7 g (68 mmol) of triethylamine, and 24 mL of DMF were then added to the flask. The mixture was heated at 80 °C for 1 h during which time a black precipitate formed. The precipitate was removed by filtration and dried to give a green brown solid residue, which was purified by flash chromatography on silica gel using 3:7 hexane:ethyl acetate solution, then recrystallized from dichloromethane−hexane to give 4.42 g (60% yield) of **8** as colorless crystals (mp 104−105 °C). HRMS (FAB, nitrogenzylalcohol matrix): calcd for MH^+ 633.2493, found 633.2473. ^{1}H NMR (500 MHz, $CDCl_3$): δ 0.37 (s, 18H), δ 1.40 (t, $J = 6.0$ Hz, 3H), δ 4.34 (q, $J = 6.0$ Hz, 2H), δ 7.11 (d, $J = 13.3$ Hz, 1H), δ 7.65 (s, 1H), δ 7.67 (s, 1H), δ 7.98 (d, $J = 13.3$ Hz, 1H), δ 8.13 (s, 1H), δ 8.14 (s, 1H). ^{13}C NMR (500 MHz, $CDCl_3$): δ −0.5, 14.6, 60.8, 110.6, 111.3, 111.6, 119.4, 121.7, 123.3, 124.8, 125.9, 127.4, 132.8, 133.8, 135.0, 140.0, 144.3, 155.2, 157.1, 167.6.

3-[6-(2-Ethoxycarbonyl-ethyl)-2,8-bis-trimethylsilanyl-dibenzofuran-4-yl]-propionic Acid (9). The synthesis of **9** was carried out similar to that of **8**. Acrylic acid (0.48 g, 6.4 mmol) was allowed to react with **8** (4.0 g, 6.4 mmol), tri-*o*-tolylphosphine (0.58 g, 1.99 mmol), and palladium(II)acetate (0.14 g, 0.64 mmol). After flash column chromatography on silica gel using 3:7 hexane:ethyl acetate as eluent, 2.76 g (90%) of the desired product (**9**) was obtained as a colorless oil. HRMS (MALDI-FTMS): calcd for MNa^+ 503.1680, found 503.1688. ^{1}H NMR (500 MHz, $CDCl_3$): δ 0.40 (s, 18H), δ 1.46 (t, $J = 5.9$ Hz, 3H), δ 4.38 (q, $J = 5.9$ Hz, 2H), δ 7.12 (d, $J = 13.4$ Hz, 1H), δ 7.15 (d, $J = 13.4$ Hz, 1H), δ 7.73 (s, 1H), δ 7.75 (s, 1H), δ 8.04 (d, $J = 13.4$ Hz, 1H), δ 8.14 (d, $J = 13.4$ Hz, 1H), δ 8.15 (s, 1H), δ 8.17 (s, 1H). ^{13}C NMR (500 MHz, $CDCl_3$): δ −0.6, 14.5, 61.0, 119.2, 119.6, 121.2, 122.1, 124.1, 124.3, 127.5, 128.0, 133.8, 134.5, 135.9, 139.1, 141.8, 155.1, 167.4, 172.7.

3-[6-(2-Ethoxycarbonyl-vinyl)-2,8-bis-trimethylsilanyl-dibenzofuran-4-yl]-acrylic Acid (10). In a 500 mL Parr hydrogenation bottle, **9** (2.76 g, 5.8 mmol) was dissolved in 100 mL of methanol and mixed with 50 mg of 10% palladium on activated carbon. The suspension was agitated under 50 psi of hydrogen at room temperature for 16 h.

The solution was filtered, and the solvent was removed under reduced pressure, affording **10** as a yellow residue (2.76 g, 100% yield). HRMS (MALDI-FTMS): calcd for MNa^+ 507.1993, found 507.1994. ^1H NMR (500 MHz, $CDCl_3$): δ 0.35 (s, 18H), δ 1.23 (t, $J = 6.0$ Hz, 3H), δ 2.84 (t, $J = 6.6$ Hz, 2H), δ 2.89 (t, $J = 6.6$ Hz, 2H), δ 3.33 (t, $J = 6.4$ Hz, 2H), δ 3.35 (t, $J = 6.4$ Hz, 2H), δ 4.15 (q, $J = 6.0$ Hz, 2H), δ 7.40 (s, 1H), δ 7.41 (s, 1H), δ 7.98 (s, 1H), δ 7.98 (s, 1H). ^{13}C NMR (500 MHz, $CDCl_3$): δ −0.7, 14.2, 25.6, 25.9, 34.1, 34.5, 60.7, 123.5, 123.7, 123.8, 123.9, 124.1, 132.1, 132.2, 134.4, 155.1, 173.6, 178.0.

3-(6-Iodo-2,8-bis-trimethylsilanyl-dibenzofuran-4-yl)-acrylic Acid Ethyl Ester (11). A dry 50 mL round-bottom flask was charged with 2.6 g (5.4 mmol) of **10**, 40 mL of benzyl alcohol, 0.56 g (5.4 mmol) of triethylamine, and 1.78 g (6.4 mmol) of dipheynylphosphonic azide. The solution was heated at reflux for 24 h and cooled to room temperature. The solvent was removed under reduced pressure, and the resulting oil was dissolved in ether (40 mL). This solution was washed with 2 M citric acid (3 × 30 mL), 5% sodium bicarbonate (3 × 30 mL), and water (2 × 40 mL). The organic layer was dried (sodium sulfate) and concentrated to afford **11** (2.22 g, 70% yield) as a pale yellow oil. HRMS (MALDI-FTMS): calcd for MNa^+ 612.2572, found 612.2566. ^1H NMR (500 MHz, $CDCl_3$): δ 0.35 (s, 18H), δ 1.21 (t, $J = 5.9$ Hz, 3H), δ 2.81 (t, $J = 6.5$ Hz, 2H), δ 3.22 (t, $J = 6.5$ Hz, 2H), δ 3.31 (t, $J = 6.5$ Hz, 2H), δ 3.67 (t, $J = 6.5$ Hz, 2H), δ 4.12 (q, $J = 5.9$ Hz, 2H), δ 5.09 (s, 2H), δ 7.29 (m, 5H), δ 7.39 (s, 1H), δ 7.40 (s, 1H), δ 7.98 (s, 1H), δ 7.99 (s, 1H). ^{13}C NMR (500 MHz, $CDCl_3$): δ −0.5, 14.4, 25.7, 30.9, 34.5, 41.2, 60.7, 66.8, 122.3, 123.9, 124.0, 124.1, 124.2, 124.4, 128.2, 128.6, 132.3, 133.0, 134.7, 134.8, 136.8, 155.4, 155.6, 156.5, 173.2.

3-[6-(2-Benzyloxycarbonylamino-ethyl)-2,8-diiodo-dibenzofuran-4-yl]-propionic Acid Ethyl Ester (12). An oven-dried 50 mL round-bottom flask was charged with 1.27 g (2.0 mmol) of **11** and 1.10 g (8.0 mmol) of K_2CO_3 and purged with nitrogen. After **11** was dissolved using 20 mL of carbon tetrachloride, the suspension was cooled to 0 °C. To the suspension was added 1.30 g (8.0 mmol) of iodine monochloride in 10 mL of carbon tetrachloride via syringe. The mixture was stirred at 0 °C for 1 h and was poured into a solution of 3 g of $NaHSO_3$ in 50 mL of water. The mixture was stirred at room temperature for 1 h, and the CCl_4 was collected. Removal of CCl_4 afforded a white precipitate, which was collected by filtration. Recrystallization from benzene−hexane gave 1.41 g (95%) of **12** as colorless crystals (mp 199−201 °C). HRMS (MALDI-FTMS): calcd for MNa^+ 719.9714, found 719.9718. ^1H NMR (500 MHz, $CDCl_3$): δ 1.21 (t, $J = 5.9$ Hz, 3H), δ 2.75 (t, $J = 6.4$ Hz, 2H), δ 3.14 (t, $J = 6.4$ Hz, 2H), δ 3.20 (t, $J = 6.4$ Hz, 2H), δ 3.63 (t, $J = 6.4$ Hz, 2H), δ 4.12 (q, $J = 5.9$ Hz, 2H), δ 4.96 (br s, 1H), δ 5.07 (s, 2H), δ 7.29 (m, 5H), δ 7.59 (s, 1H), δ 7.59 (s, 1H), δ 8.05 (s, 1H), δ 8.07 (s, 1H). ^{13}C NMR (500 MHz, $CDCl_3$): δ 14.2, 24.8, 30.3, 33.8, 40.6, 60.6, 66.7, 86.3, 125.2, 125.3, 127.0, 128.0, 128.0, 128.1, 128.2, 128.5, 136.2, 136.7, 154.0, 154.2, 156.2, 172.4.

3-[6-(2-Benzyloxycarbonylamino-ethyl)-8-(2-*tert*-butoxycarbonyl-vinyl)-4-(2-ethoxycarbonyl-ethyl)-dibenzofuran-2-yl]-acrylic Acid *tert*-Butyl Ester (13). The synthesis of **13** was similar to that of **8**. *tert*-Butyl acrylate (0.44 g, 3.44 mmol) was allowed to react with **12** (1.2 g, 1.72 mmol), tri-*o*-tolylphosphine (0.16 g, 0.53 mmol), and palladium(II)acetate (20 mg, 0.17 mmol). After flash column chromatography on silica gel using 3:7 hexane:ethyl acetate solution as eluent, the desired product (**13**) was obtained (0.96 g, 80% yield) as a colorless oil. HRMS (MALDI-FTMS): calcd for MNa^+ 720.3143, found 720.3156. ^1H NMR (500 MHz, $CDCl_3$): δ 1.21 (t, $J = 5.9$ Hz, 3H), δ 1.56 (s, 18H), δ 2.79 (t, $J = 6.4$ Hz, 2H), δ 3.20 (t, $J = 6.4$ Hz, 2H), δ 3.28 (t, $J = 6.4$ Hz, 2H), δ 3.67 (t, $J = 6.4$ Hz, 2H), δ 4.12 (q, $J = 5.9$ Hz, 2H), δ 5.07 (s, 2H), δ 6.42 (d, $J = 3.8$ Hz, 1H), δ 6.45 (d, $J = 3.8$ Hz, 1H), δ 7.29 (m, 5H), δ 7.46 (s, 1H), δ 7.47 (s, 1H), δ 7.68 (s, 1H), δ 7.71 (s, 1H), δ 7.93 (s, 1H), δ 7.94 (s, 1H). ^{13}C NMR (500 MHz, $CDCl_3$): δ 14.4, 25.3, 28.4, 30.8, 34.1, 40.9, 60.8, 66.8, 80.7, 119.1, 119.3, 119.8, 120.0, 124.7, 125.4, 127.7, 128.2, 128.3, 128.7, 130.5, 130.6, 136.7, 143.4, 143.5, 156.1, 156.3, 156.5, 166.5, 166.5, 172.8.

3-{2,8-Bis-(2-*tert*-butoxycarbonyl-ethyl)-6-[2-(9*H*-fluoren-9-yl-methoxycarbonylamino)-ethyl]-dibenzofuran-4-yl}-propionic Acid (4). Hydrolysis, hydrogenation, and Fmoc protection of the amino group were carried out consecutively using the crude product from the previous step. Hydrolysis was performed by dissolving 0.32 g (0.47 mmol) of **13** in 10 mL of 3:1 tetrahydrofuran:ethanol to which was added 2.5 mL of 1 M LiOH in water. The reaction was complete after 12 h. The mixture was neutralized utilizing dilute HCl and diluted with 50 mL of dichloromethane. The aqueous layer was separated, and the organic layer was dried ($MgSO_4$). The solvent was removed under reduced pressure. The crude residue was subjected to hydrogenation as described previously for the preparation of **10** (10 mL of methanol with 5 mg of 10% palladium on activated carbon). The crude product from hydrogenation was dissolved in 10 mL of dichloromethane, and Fmoc-OSu (0.23 g, 0.7 mmol) was added. The mixture was stirred at room temperature for 12 h, and the solvent was removed under reduced pressure. The desired product **4** was purified by flash column chromatography (7:3 hexane:ethyl acetate), affording **4** as a white foam (0.34 g, 95% yield for these three steps combined). HRMS (MALDI-FTMS): calcd for MNa^+ 784.3456, found 784.3449. ^1H NMR (500 MHz, $CDCl_3$): δ 1.40 (s, 18H), δ 2.53 (t, $J = 7.5$ Hz), δ 2.61 (m, 3H), δ 2.65 (m, 1H), δ 2.83 (m, 1H), δ 2.95 (t, $J = 6.4$ Hz, 1H), δ 3.02 (m, 3H), δ 3.14 (m, 2H), δ 3.30 (m, 2H), δ 3.62 (m, 2H), δ 4.03 (m, 0.5H), δ 4.07 (m, 1H), δ 4.18 (m, 0.5H), δ 4.40 (m, 1H), δ 5.17 (m, 0.5H), δ 6.78 (m, 0.5H), δ 7.11 (m, 2H), δ 7.26 (t, $J = 6.2$ Hz, 2H), δ 7.37 (t, $J = 6.2$ Hz, 2H), δ 7.42 (m, 1H), δ 7.53 (m, 1H), δ 7.59 (t, $J = 5.2$ Hz, 2H), δ 7.73 (t, $J = 5.2$ Hz, 2H). ^{13}C NMR (500 MHz, $CDCl_3$): δ 26.5, 27.0, 28.1, 29.5, 31.0, 36.4, 37.7, 41.2, 43.3, 47.0, 47.1, 67.0, 67.5, 80.4, 118.5, 119.9, 125.0, 127.0, 127.7, 128.0, 128.4, 135.5, 135.6, 135.7, 141.2, 141.3, 143.6, 143.8, 153.6, 153.7, 153.8, 154.3, 156.4, 158.5, 172.3.

General Method for Solid-Phase Peptide Synthesis (SPPS). Automated solid-phase peptide synthesis was performed on an Applied Biosystems 433A peptide synthesizer. All syntheses were performed on a 0.1 mmol scale using the standard Fmoc-based FastMoc coupling chemistry provided by the system's software. Briefly, the coupling reactions were carried out in *N*-methylpyrrolidone (NMP) using 10 equiv of amino acid and the activating agents 2-(1*H*-benzotriazol-1-yl)-1,1,3,3 tetramethyluronium hexafluorophosphate (10 equiv) and 1-hydroxybenzotriazole (10 equiv) in the presence of diisopropylethylamine (10 equiv). The N-terminal Fmoc deprotection was achieved using 20% piperidine in DMF for 20 min. The templates **1a** and **1b** (1.2 equiv) were incorporated manually using 1.2 equiv of the activating agents HBTU/HOBt in DMF (2 mL) in the presence of 2.2 equiv of diisopropylethylamine (2 M in NMP). The coupling was carried out for 24 h before loading the resin back on the synthesizer for further extension of the peptide chain. Peptide cleavage and side-chain deprotection were carried out by gently agitating the crude peptide-resin in Reagent K (1 mL per 0.025 mmol of crude peptide) (Reagent K: 82.5% TFA, 5% *m*-cresol, 5% thioanisole, 5% water, and 2.5% EDT) for 2 h at room temperature. Crude peptide was precipitated in *tert*-butyl methyl ether, centrifuged, redissolved in DMF, and purified by HPLC using a 10−50% linear gradient in solvent B over 60 min.

CD Studies. CD spectra were recorded using an Aviv model 202SF circular dichroism spectrometer equipped with a Peltier temperature-controlled cell holder using a 0.2 cm path length Suprasil quartz cell (Hellma, Forest Hills, New York). Far-UV CD spectra were recorded from 200 to 250 nm at 2 and 25 °C. The wavelength step size was 0.5 nm, and the averaging time used was 2 s per scan at each wavelength step. The peptide sample was dissolved in 20 μM sodium phosphate (pH 7.0). Thermal denaturation was monitored at 227 nm. The temperature range utilized was from 2 to 98 °C with a 2 °C step size with a 90 s equilibration time. Data for each point were averaged for

30 s. After the highest temperature was reached, the sample was cooled to 25 °C, and another wavelength scan was taken. Fraction unfolding (f_u) was determined using the baseline extrapolation method. T_m was determined from the fraction unfolding curve (T_m = temperature at which $f_u = 0.5$) as previously described.[16]

Guanidinium hydrochloride (GuHCl) denaturation was accomplished using the automated titrator accessory on the Aviv instrument model 202SF. Two solutions were prepared, the first being 5 μM protein in 20 μM sodium phosphate buffer at pH 7.0, and the second 5 μM protein in 7 M GuHCl (20 μM sodium phosphate buffer at pH 7.0). The second solution was added to the first in steps such that the denaturant concentration of the mixture increased by 0.2 M/step, while the protein concentration remained fixed. The equilibration time was fixed to 10 min for each addition with constant stirring. The data were collected at 227 nm with a 30 s average time at 4 °C. The denaturation curves were analyzed assuming two-state behavior using a previously described method.[16]

Analytical Ultracentrifugation. The solution molecular weights of the peptides were evaluated by sedimentation equilibrium measurements carried out with a temperature-controlled Beckman XL-I Analytical Ultracentrifuge equipped with an An-60 Ti rotor and a photoelectric scanner (Beckman Instrument Inc., Palo Alto, CA). Protein samples (100 μM in 20 μM sodium phosphate (pH 7.0)) were loaded in a double sector cell equipped with a 12 mm Epon centerpiece and a sapphire optical window. The reference compartment was loaded with the matching 20 μM sodium phosphate (pH 7.0). The samples were monitored at 280 nm at a rotor speed of 3000−40 000 rpm at 20 °C and analyzed by a nonlinear squares approach using Origin (Microcal Software Inc., Northampton, MA). The data were fit to the Lamm equation for a single species model

$$A_r = A_0 \exp[\omega^2/2RT^*M(1 - \bar{v}\rho)](r^2 - r_0^2) \quad (1)$$

where A_r is radial absorbance, A_0 is the baseline absorbance, ω is the rotor speed (s^{-1}), R is the gas constant (J mol^{-1} K^{-1}), T is the temperature (K), $\bar{v}$ is the partial specific volume (mL g^{-1}), ρ is the density of solvent (g mL^{-1}), r is the variable radius, and r_0 is the meniscus radius. The hydrodynamic masses of all the peptides synthesized in this study are summarized in Table 2. Note that a mass for Peptide **A** could not be obtained because of the formation of large aggregates.

Acknowledgment. We gratefully acknowledge financial support from NIH (GM 51105), The Skaggs Institute of Chemical Biology, and The Lita Annenberg Hazen Foundation, and helpful discussions with Professor Evan T. Powers.

Supporting Information Available: ^1H and ^{13}C NMR spectra for all new compounds synthesized in this paper (PDF). This material is available free of charge via the Internet at http://pubs.acs.org.

JA020675X